MEMO TO: File

FROM: H. A. Wheeler

SUBJECT: The Goubau design of a disc-loaded monopole.

Abstract. The Goubau design of a disc-loaded monopole is characterized by a disc divided into 4 sectors on 4 posts, 2 for support and 2 for feed connections. Its impedance matching has been measured and is presented on the reflection chart. Its configuration in each quadrant is described in terms of lumped reactors. It is reduced to an equivalent ladder network, for ease of computation. Triple tuning becomes apparent, in accord with the measured locus.

The subject antenna is a rather small disc-loaded monopole left by the late Dr. Georg Goubau. It has some peculiar structural features for integrated wideband matching by fixed tuning. Over a frequency-bandwidth ratio of about 1:2 (450-900 Mhz) it only marginally qualifies as a "small antenna". The matching efficiency over this band is comparable with what would be expected from a simple disc-loaded monopole of the same size, with a fixed matching network.

The Goubau design has a disc divided into four sectors on posts, two for support and two for feed connection. See Fig. 1. The sectors are interconnected by short wires. The rationale for the design is not apparent and now may never be known. It has some similarity to a folded monopole.

Its performance is remarkable for an integrated structure. It is measured by the reduction of VSWR over the band, or the inversely related matching efficiency. See Fig. 2. He may have thought that this design would exceed the fundamental limitations formulated for a small antenna of its size. However, nearly equal matching efficiency has been demonstrated by a design with a simple disc of equal diameter and height, having integrated matching with comparable circuit complexity. This is the subject of another memo.

The performance of the model can be computed to any degree of approximation by the laborious numerical method of moments. (This would ignore the small effect of the dielectric sheet supporting the disc sectors.) One such exercise has yielded a similar impedance locus.

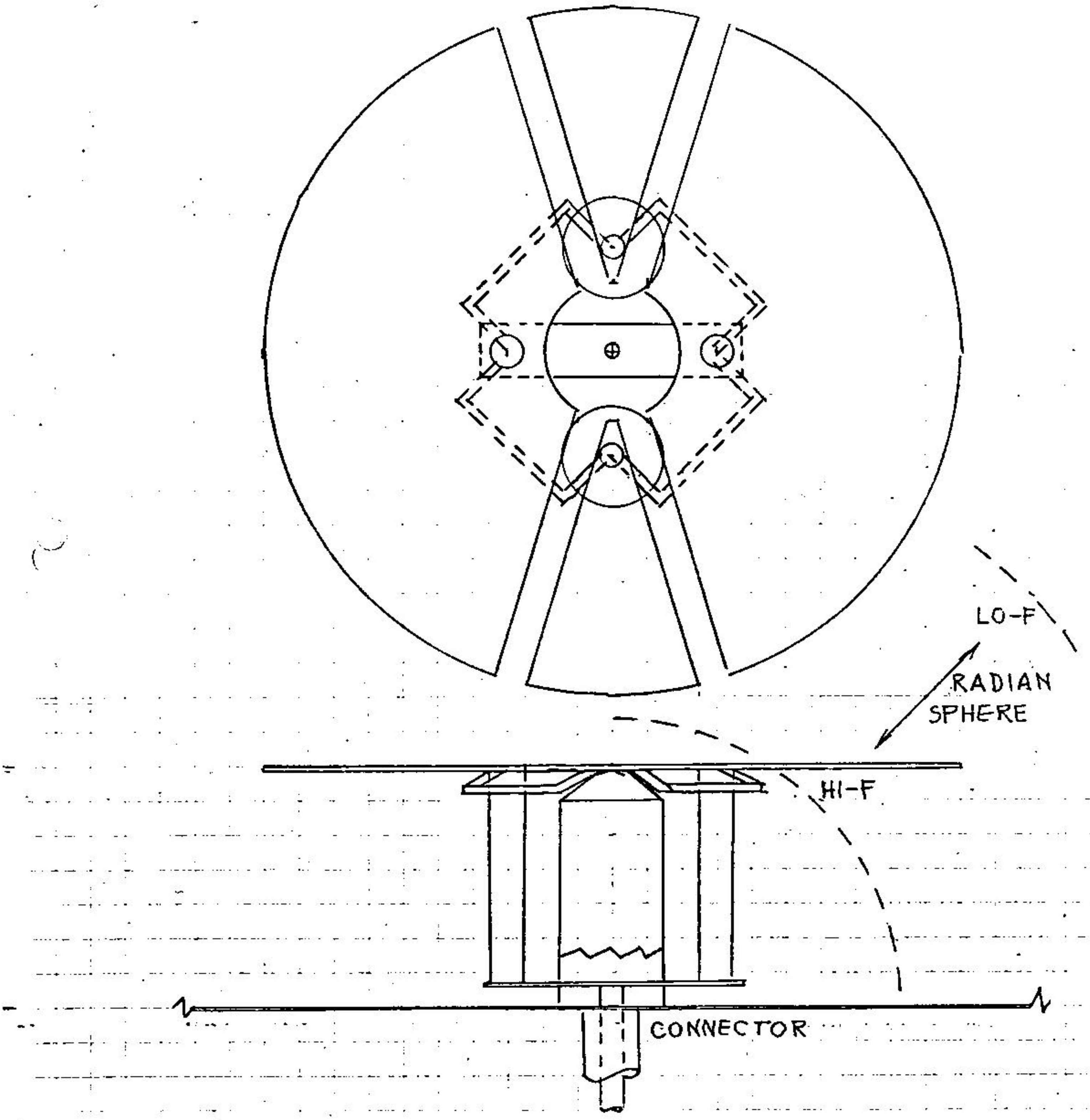

Fig. 1 - Structure of Goubau design (full-size).

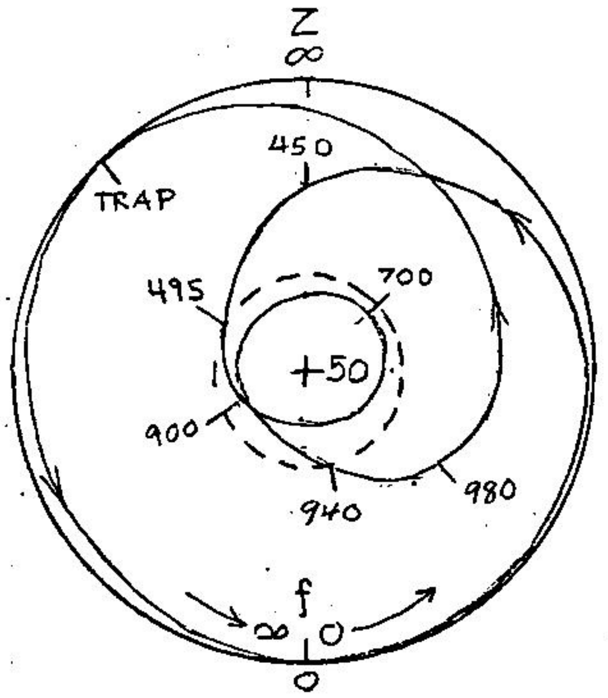

(a) Reflection locus.

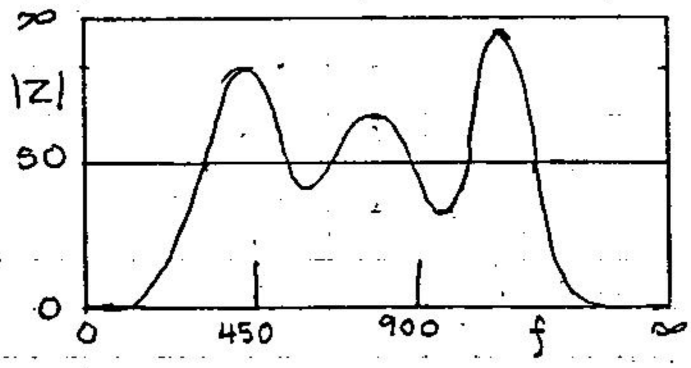

(b) Impedance graph.

Fig. 2 - Triple tuning shown by impedance plots.

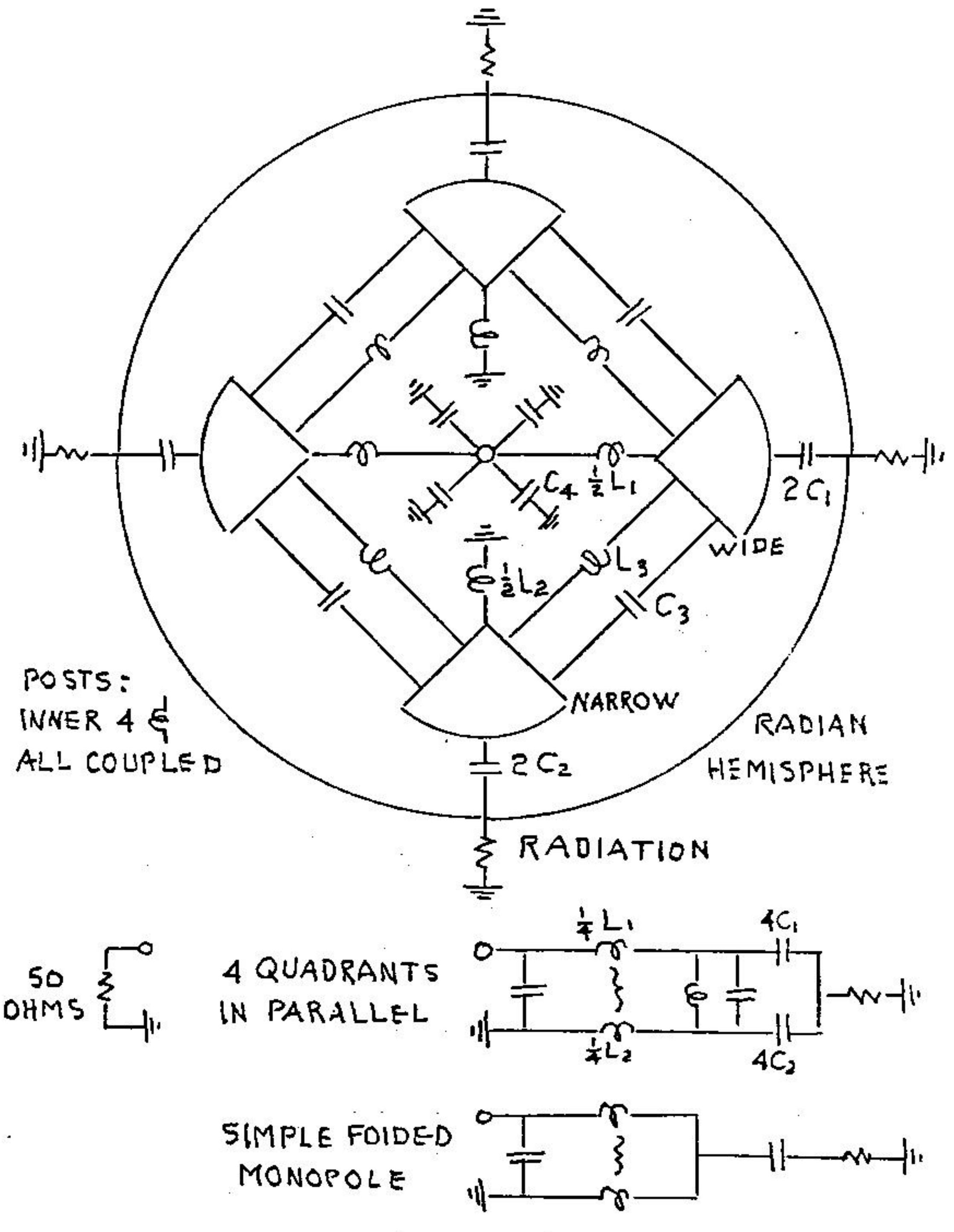

Fig. 3 - Circuit representation of the structure.

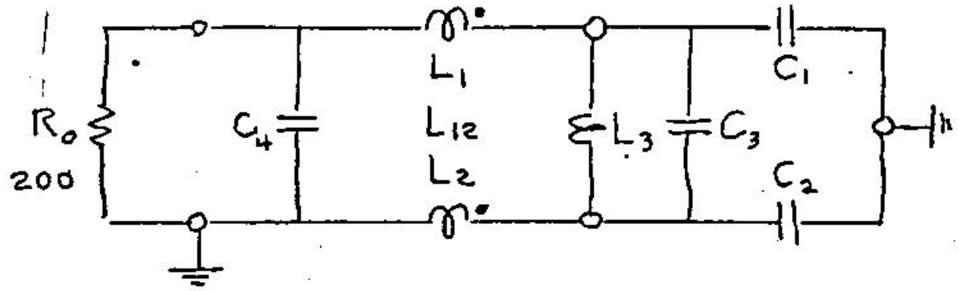

Fig. 4 - Circuit reactors in one quadrant.

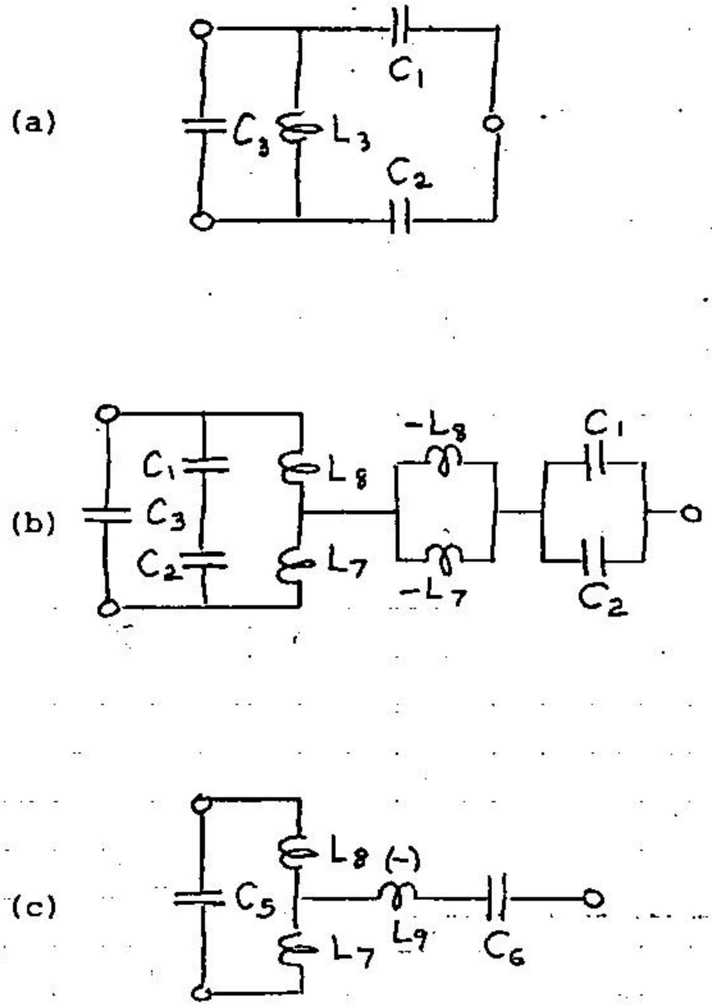

Fig. 5 - Circuit equivalent of disc sectors and interconnecting wire in one quadrant.

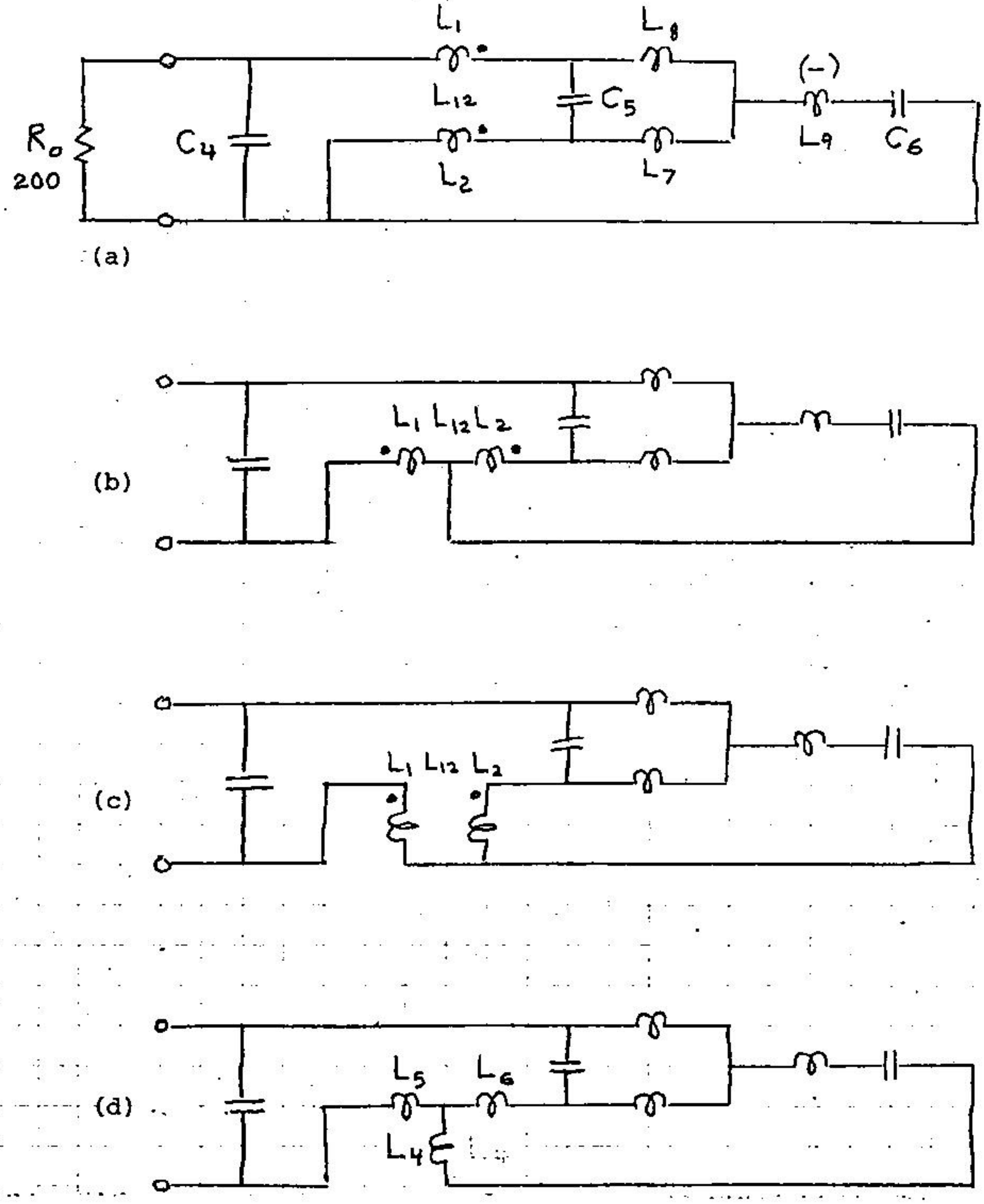

Fig. 6 - Circuit transformation to ladder and bridged-T sections.

(e)

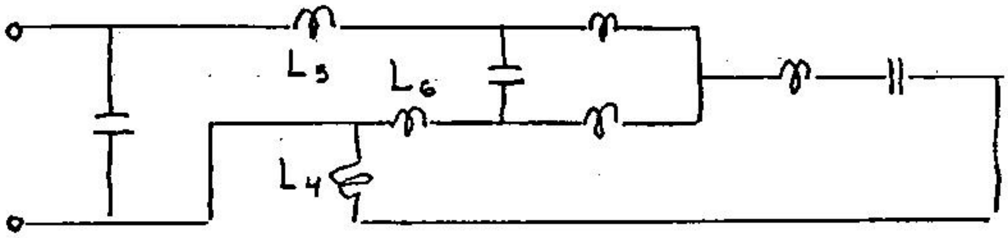

(f)

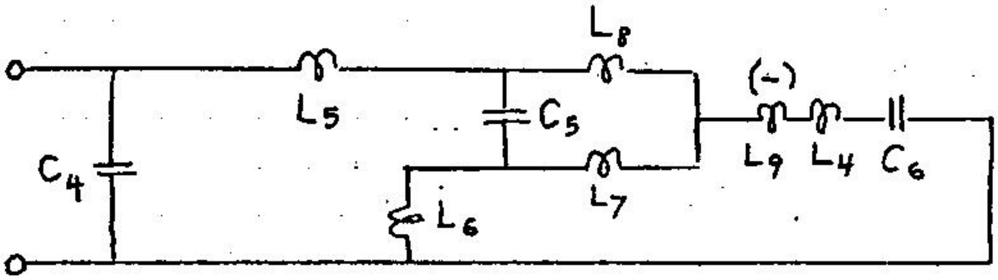

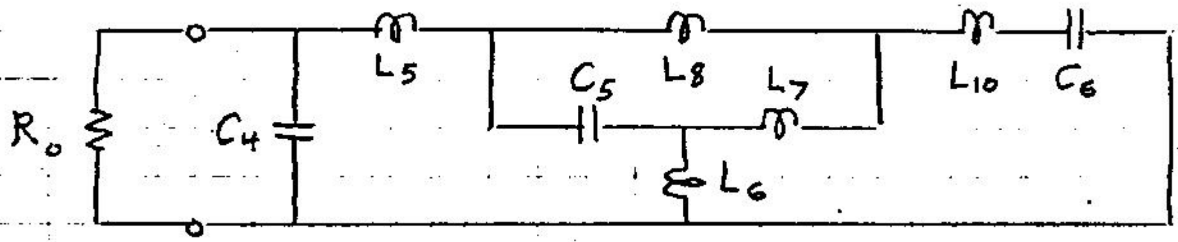

(g)

Fig. 6 - continued.

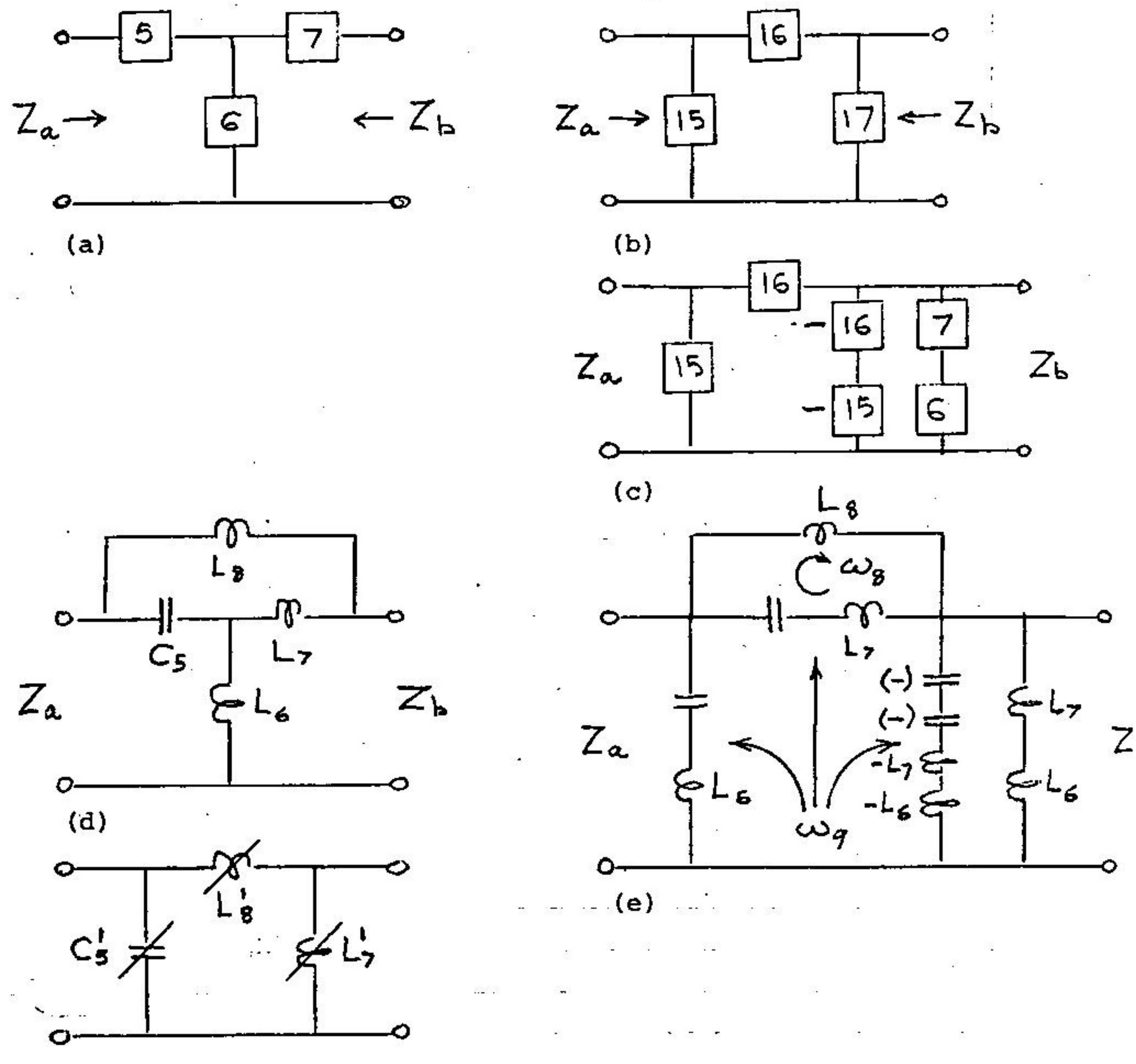

Fig. 7 - Transformation of bridged-T section to equivalent ladder section.

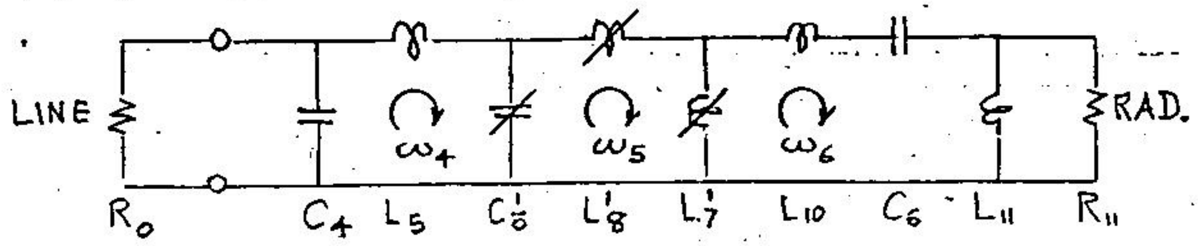

Fig. 8 - Complete circuit representation in ladder form, showing triple tuning.

Fig. 1 is a diagram (full size) of the essential features of the Goubau model for 450-900 Mhz. It has four identical quadrants bounded by orthogonal planes of symmetry. They are in parallel with respect to their electromagnetic behavior and their circuit representation, as will be seen. The disc is divided into two unequal pairs of sectors.

Fig. 2 shows graphs of the impedance behavior over the frequency domain, based on measurements. The reflection locus (a) goes 3 times around, which is a test for triple-tuning. Within the dashed tolerance circle (VSWR = 2) the locus goes somewhat more than 2 times around, indicating the utilization of more than double tuning. The locus within the circle is rather close to the circle, which is one test of "effective" matching by saturating the tolerance. The impedance graph (b) has 3 peaks in or near the nominal frequency band, which is another view of the test for triple tuning.

Fig. 3 is an analysis of the structure in terms of circuit elements representing the electromagnetic behavior. In one quadrant, the elements are identified for further study. The circuit diagram is intended to indicate the essentials of the 4 quadrants operating in parallel. The radiation is simulated by terminating the circuit on the surrounding radiansphere.

Fig. 4 shows the reactors in one quadrant, identified for further analysis.

- C_1 and C_2 are the adjacent (wide and narrow) half-sectors of the quarter-disc.
- L_3 is the interconnecting wire.
- L_1 and L_2 are the coupled (narrow and wide) half-posts for electrical connection and mechanical support.
- R_o is the quadrant resistance of the connecting cable (4 × 50 ohms).

Fig. 5 shows a transformation to place the total disc C in one branch. For equivalence, one can see these relations:

$$C_6 = C_1 + C_2 \; ; \quad L_7 + L_8 = L_3 \; ; \quad L_7/L_8 = C_1/C_2 \qquad (1)$$

$$C_5 = C_3 + \frac{C_1 C_2}{C_1 + C_2} \qquad (2)$$

$$L_7 = L_3 \frac{C_1}{C_1+C_2} \; ; \; L_8 = L_3 \frac{C_2}{C_1+C_2} \; ; \; L_9 = \frac{-L_7L_8}{L_7+L_8} \qquad (3)$$

The negative L_9 provides "close coupling" in L_7, L_8.

Fig. 6 shows a rearrangement from the coupled inductors (L_1,L_2) to a bridged-T of self-reactors.

$$L_4 = L_{12} \; ; \; L_5 = L_1 - L_{12} \; ; \; L_6 = L_2 - L_{12} \qquad (4)$$

$$L_{10} = L_4 + L_9 = L_4 - \frac{L_7L_8}{L_7+L_8} \qquad (5)$$

All of these may be positive and hence realizable as separate physical inductors. They will be regarded as positive for further development.

Fig. 7 shows the transformation from T to Π, then the addition of the bridge and the description in equivalent ladder arms, in this order:

(a) The T in general terms;
(b) The Π to be made equivalent;
(c) One form of equivalent Π, which is suited for present purposes as will be seen;
(d) The bridged-T of reactors as seen in Fig. 6 (g);
(e) The equivalent Π in terms of reactors (some negative);
(f) The ladder arms in terms of frequency-variant positive reactors, effective in the operating band.

In Fig. 7(a) and (b), the familiar transformation gives these formulas.

$$Z_{15} = Z_5 + Z_6 + Z_5Z_6/Z_7 = Z_6 + Z_5(1 + Z_6/Z_7) \qquad (6)$$

$$Z_{16} = Z_5 + Z_7 + Z_5Z_7/Z_6 = Z_7 + Z_5(1 + Z_7/Z_6) \qquad (7)$$

$$Z_{17} = Z_6 + Z_7 + Z_6Z_7/Z_5 \qquad (8)$$

In the present network, from Fig. 6(g), Z_{15} and Z_{16} are physically realizable because Z_6/Z_7 is a constant. This is not true of Z_{17}, so it will be described by including negative elements.

Referring to Fig. 7(a) and (c), Z_b(OC) denotes Z_b with the opposite end on open circuit. By dividing Z_{17} in parallel negative and positive branches as shown in Fig. 7(c), the negative branch nullifies Z_{16} and Z_{17} in the Π. Then the positive branch is equal to the sum of Z_6 and Z_7 in the T, independent of Z_5. The Z_{17} arm is thereby represented by parallel branches of positive and negative circuit elements.

Fig. 7(d) and (e) show the actual bridged-T from Fig. 6(g) and its equivalent represented in the manner of Fig. 7(c).

A critical frequency (ω_9) is identified with a zero of Z_a(SC) or Z_b(SC).

$$\omega_9^2 = (L_6+L_7)/C_5L_6L_7 \qquad (9)$$

This is a resonance for both ends on short circuit (SC). All 3 arms of the Π are zero at this frequency, so its behavior is indeterminate. In the usual manner, it can be resolved in the limit of $\omega \to \omega_9$. In Fig. 7(e), this frequency and the L values provide a complete description of each arm. From (8) or Fig. 7(e), the frequency variation of the composite arm is:

$$Z_{17} = j\omega(L_6+L_7)(1-\omega^2/\omega_9^2) \qquad (10)$$

While not physically realizable in the ladder configuration, this formula is convenient for computation by the simple ladder algorithm.

Another critical frequency ($\omega_8 < \omega_9$) is identified with an infinity of the composite series arm formed of Z_{16} "bridged" by L_8.

$$\omega_8^2 = \omega_9^2L_7/(L_7+L_8) = (L_6+L_7)/C_5L_6(L_7+L_8) < \omega_9^2 \qquad (11)$$

This is an "anti-resonance" or "trap frequency" of zero transmission. On the hemisphere chart of reflection, Fig. 2(a), this frequency is identified with a point of tangency on the rim of the chart, corresponding to complete reflection. This and hence also ω_9 occur at frequencies above the operating band.

Fig. 7(f) shows the behavior of this bridged-T in the operating band (below ω_8 and ω_9). Each reactor is shown as a frequency-variant single positive element.

$$C_5' = \frac{C_5}{1-\omega^2/\omega_9^2} \cdot \frac{L_7}{L_6+L_7} \tag{12}$$

$$L_7' = (L_6+L_7)(1-\omega^2/\omega_9^2) \tag{13}$$

$$L_8' = L_8(1-\omega^2/\omega_9^2)/(1-\omega^2/\omega_8^2) \tag{14}$$

Fig. 8 shows the entire network of Fig. 6(g) with the bridged-T replaced by the ladder arms of frequency-variant elements. Triple tuning is implied by 3 meshes coupled along the ladder network. Their 3 frequencies of resonance (ω_4, ω_5, ω_6) can be computed from the coefficients, although the middle one requires the solution of a cubic equation. The radiation is simulated by a constant R_{11} across L_{11}, which is a fair approximation.

A remarkable result of the bridged-T is the reactance variation of L_7' in series with C_6. The natural slope of the latter is decreased by the former. This would tend to increase the radiation bandwidth in the ω_6 mesh including the radiator. The expected result would be closer wideband matching than could be obtained with a ladder network of equal complexity.

One reservation in this representation is the marginal qualification as a small antenna. Fig. 1 shows to scale the radiansphere at the extremes of the frequency band. The smaller sphere does not enclose all the structure, so the "small antenna" theory becomes incomplete.